ISBN: 978-3-95450-227-1 ISSN: 2673-5490 doi:10.18429/JACoW-IPAC2022-WEPOMS037

MICROBUNCHING STUDIES FOR THE FLASH2020+ UPGRADE USING A SEMI-LAGRANGIAN VLASOV SOLVER

Ph. Amstutz* and M. Vogt
Deutsches Elektronen-Synchrotron DESY, Germany

Abstract

Precise understanding of the microbunching instability is mandatory for the successful implementation of a compression strategy for advanced FEL operation modes such as the EEHG seeding scheme, which a key ingredient of the FLASH2020+ upgrade project. Simulating these effects using particle-tracking codes can be quite computationally intensive as an increasingly large number of particles is needed to adequately capture the dynamics occurring at small length scales and reduce artifacts from numerical shot-noise. For design studies as well as dedicated analysis of the microbunching instability semi-Lagrangian codes can have desirable advantages over particle-tracking codes, in particular due to their inherently reduced noise levels. However, rectangular high-resolution grids easily become computationally expensive. To this end we developed SelaV$_{1D}$, a one dimensional semi-Lagrangian Vlasov solver, which employs tree-based domain decomposition to allow for the simulation of entire exotic phase-space densities as they occur at FELs. In this contribution we present results of microbunching studies conducted for the FLASH2020+ upgrade using SelaV$_{1D}$.

INTRODUCTION

In the injector and linac sections upstream of the undulators of an free-electron laser (FEL), collective interaction of the electrons in a bunch can – in combination with longitudinal dispersion in parts of the beamline – lead to the formation of substructures in the longitudinal phase-space density (PSD) of the bunch [1]. This so-called microbunching instability (MBI) can have significant impact on the efficacy of free-electron lasers, due to the resulting increase of the energy spread and enhanced irregularities in the longitudinal phase-space and in the current density [2]. Hence, during the design of new FEL injectors, care has to be taken to ensure the setup does not produce a microbunching gain beyond tolerable levels. While leading-order theories for the gain function of the MBI exist, simulations are still required to study the full dynamics of the instability and capture also non-linear effects. We present studies of the MBI for the FLASH2020+ upgrade project [3], conducted with SelaV$_{1D}$ [4], a semi-Lagrangian code in one degree of freedom, which employs tree-based domain decomposition to enable the simulation of an entire bunch on all relevant length scales [5]. The semi-Lagrangian approach yields a smooth solution [6] of the Vlasov equation and hence allows to efficiently study the MBI without the artificial shot-noise that is inherent to macroparticle simulation codes.

* philipp.amstutz@desy.de

COMPRESSION WORKING POINTS

The injector beamline of FLASH2020+ comprises two bunch compression stages in the form of C-shape magnetic chicanes with the corresponding upstream off-crest operated RF modules, shown in Figure 1. The nominal R_{56} of the two chicanes is 139.9 mm at a beam energy of around 145 MeV and 72.6 mm at around 550 MeV, respectively. Acceleration

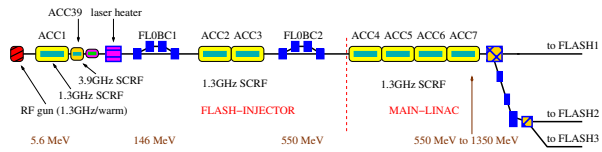

Figure 1: Layout of the injector and linac beamline of FLASH2020+.

is provided by seven accelerating modules ACC1 to ACC7, which, together with the 3.9 GHz linearizer module ACC39, yield a maximum energy of 1.35 GeV. In the focus of this

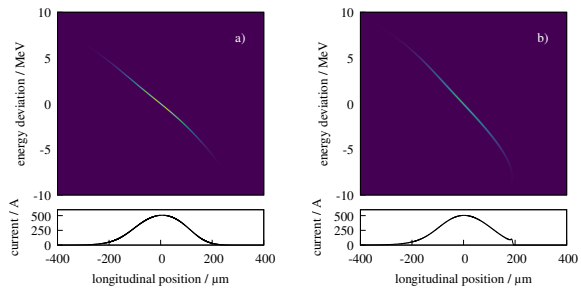

Figure 2: Longitudinal PSD and current profiles after the second chicane for a) WP1 and b) WP2.

study are two compression working points which are especially suited for the Echo-Enable Harmonics Generation (EEHG) seeding scheme, which will be employed in the FLASH1 beamline. An intermediate peak current of about 500 A is projected for EEHG operation in FLASH1. For EEHG it is particularly desirable for the electron bunch to feature a longitudinal PSD that has as small of a curvature in the central part of the bunch as possible.

To this end, two compression working points, WP1 and WP2, were chosen, as shown in Table 1. Both provide compression of a 400 pC bunch to a final current of 500 A. The final longitudinal phase-space has negligible non-linear covariance in the central part up to third order, shown in Figure 2. WP1 assumes the bunch to leave the gun with a peak current of $I_0 = 31.25$ A, which is then compressed by a factor 4 in each compression stage. For WP2 a reduced initial current of $I_0 = 20$ A is assumed, requiring stronger subse-

ISBN: 978-3-95450-227-1 ISSN: 2673-5490 doi:10.18429/JACoW-IPAC2022-WEPOMS037

quent compression by a factor 5 in both stages. In addition to the evaluation of the two compression working points the impact of increasing the energy spread of the bunch by means of the laser heater [7], which will be installed during the FLASH2020+ upgrade, is studied.

Table 1: Amplitudes in MeV and Off-Crest Phases for the Two RF Working Points

	ACC1	ACC39	ACC23
WP1	163.8, 11.87°	19.94, −175.39°	415.1, 13.27°
WP2	161.3, 12.91°	19.92, −174.23°	413.3, 10.07°

MONOCHROMATIC GAIN STUDIES

Let $\Psi_s[A,k](z)$ be the PSD of the bunch at the position s along the beamline, $z = (q,p)$ being the canonical variables representing deviation in the longitudinal position and energy respectively; with the seeded initial condition

$$\Psi_{s_0}[A,k](z) = u(z)(1 + A\ \sin(q\,k)), \tag{1}$$

where u is some well-behaved test function and k and A, $0 \leq A \leq 1$ are the wave number and amplitude of the monochromatic seeding perturbation of the longitudinal charge density. Then a measure for the growth of the MBI between two positions s_0 and s_1 is the gain function defined by

$$g_A(C,k) = \frac{\left|\tilde{\rho}_{s_1}[A,k/C](k)\right| - \left|\tilde{\rho}_{s_1}[0,0](k)\right|}{A}, \tag{2}$$

where $\tilde{\rho}$ denotes the Fourier transform of the charge density $\tilde{\rho}_s(k) \equiv \int_{\mathbb{R}^2} \Psi_s(z)\ \exp(-\mathrm{i}\,k\,q)\,\mathrm{d}^2z/\sqrt{2\pi}$, and C is a compression factor. The so-called linear gain function is then given as the limit of g_A for small perturbation amplitudes

$$g_{\mathrm{lin}}(C,k) \equiv \lim_{A\to 0} g_A(C,k). \tag{3}$$

The semi-Lagrangian approach is especially suitable to numerically calculate such a gain function, not only due to the absence of unwanted shot-noise, but also due to the fact that the numerical representation of the PSD can be directly modified, so that applying a perturbation to a test function as described by Eq. (1) is straightforward.

For the simulations presented in the following, we chose u to be the uncorrelated bivariate Gaussian function with variances σ_q^2 and σ_p^2. The simulations start at the entrance of the first module. In these simulations longitudinal space-charge (LSC) is included as the only collective effect. It should be noted that a one-dimensional model of interaction via coherent synchrotron-radiation in the magnetic chicanes [8] indeed is implemented in SelaV$_{1D}$ and its influence on the microbunching gain will be be the subject of future work. Figure 3 shows the LSC-driven linear microbunching gain functions $g_{\mathrm{lin}}(C,k)$ after the second bunch compression stage for both working points at a fixed value of the compression factor C. In both cases C was chosen close to

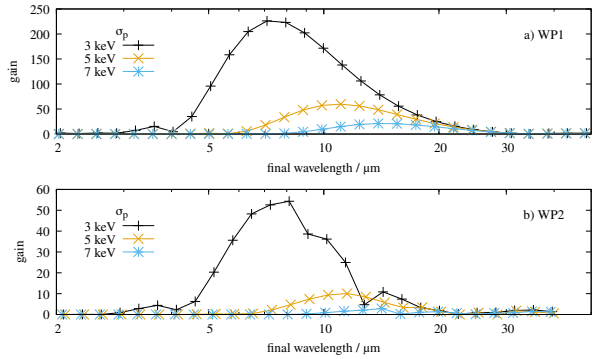

Figure 3: Microbunching gain functions for multiple values of the initial bunch energy spread at both working points a) WP1 and b) WP2.

the nominal compression of the respective working point, $C_{\mathrm{WP1}} = 16$ and $C_{\mathrm{WP2}} = 25$. To approximate the limit in Equation (3) numerically, the perturbation amplitude was chosen sufficiently small, $A = 10^{-4}$. As can be seen in Fig. 3, WP2 exhibits a significant reduction of the microbunching gain in comparison to WP1. At the nominal energy spread of $\sigma_p = 3$ keV the maximum gain occurs in the wavelength range 6 µm to 9 µm in the final charge density, independent on the working point. Increasing the initial energy spread to $\sigma_p = 7$ keV by means of the laser heater shifts the region of maximum gain to around 14 µm to 19 µm and decreases the maximum gain by an order of magnitude.

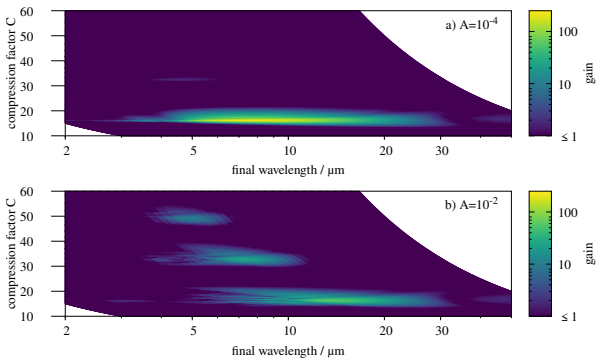

Figure 4: 2D gain functions for WP1 with $\sigma_p = 3$ keV.

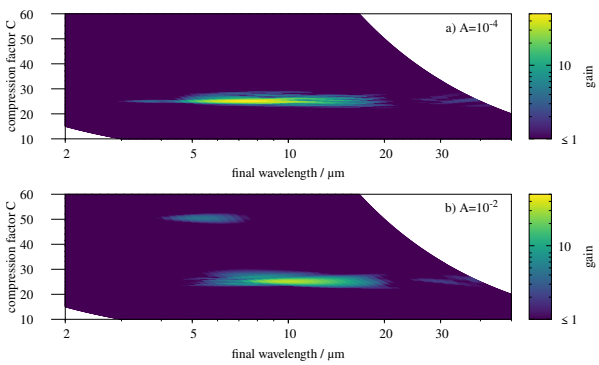

Figure 5: 2D gain functions for WP2 with $\sigma_p = 3$ keV.

ISBN: 978-3-95450-227-1 ISSN: 2673-5490 doi:10.18429/JACoW-IPAC2022-WEPOMS037

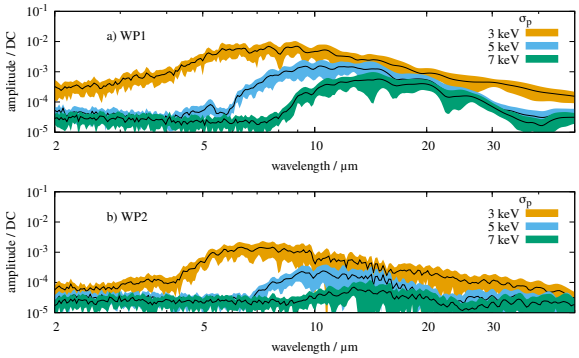

Figure 6: Average (black line) and standard deviation (colored areas) of the shot-noise induced microbunching spectra after FL0BC2 for different energy spreads at working point a) WP1 and b) WP2, respectively. The sample size is 16.

Especially for the study of non-linear effects, it proved to be insightful to keep C as a free variable and plot the gain as a function of both, the final wavelength and the compression factor. The resulting 2D gain functions reveal the potential frequency up-conversion of initial disturbances and the resulting formation of higher harmonics, as well as the bandwidth of the microbunching gain with respect to C.

Figures 4 and 5 show the 2D gain functions for WP1 and WP2 respectively, evaluated with a perturbation amplitude of $A = 10^{-4}$ and $A = 10^{-2}$. While for small perturbation amplitudes significant gain only occurs close to the nominal compression factor, at larger amplitudes the formation of harmonics around multiples of the nominal compression factor is observed.

SHOT NOISE STUDIES

In addition to the gain studies presented above, where the MBI is excited by a perturbation at a single wavelength, another insightful approach is to study the MBI developing from shot-noise, see also [9]. In a semi-Lagrangian simulation shot-noise can be incorporated in the initial PSD Ψ_0 by replacing the grid values $u_{ij} = u(z_{ij})$ of a smooth test PSD u with a random variable that locally follows a scaled Poisson distribution with parameter $\lambda(z_{ij}) = u_{ij}|Q|/e\,\mathrm{d}^2 z_{ij} = \lambda_{ij}$, where Q is the bunch charge and $\mathrm{d}^2 z_{ij}$ is the area covered by the grid cell,

$$\Psi_0(z_{ij}) = X_{ij}/\mathrm{d}^2 z_{ij}, \text{ with } P(X_{ij} = k) = \frac{\lambda_{ij}^k \mathrm{e}^{-\lambda_{ij}}}{k!}. \quad (4)$$

Statistics of the spectra of the resulting charge densities after the second bunch compression stage are shown in Figure 6. The dependence of these spectra on energy spread and compression working point are in good agreement with the results from the monochromatic gain study above. This result suggests that in a realistic bunch the charge-density perturbations induced by shot-noise are small enough so that the linear gain approximation holds.

Figure 7 shows the PSD in the central part of a bunch, highlighting the beneficial effect of larger energy spread and

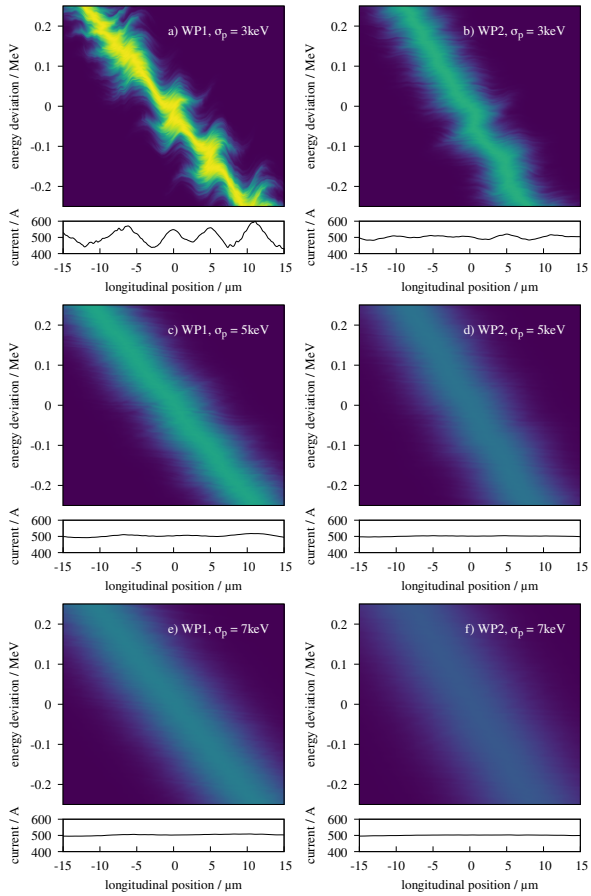

Figure 7: Examples of the phase-space density after FL0BC2 in the central part of a bunch, onto which Poisson shot-noise has been imprinted initially.

stronger compression on the suppression of microbunching structures forming from shot-noise. It can be seen that the microbunching process does not only result in inhomogeneities in the charge-density but also increases the local energy spread of the bunch.

CONCLUSION

The simulation studies presented in this contribution indicate that a well-chosen compression working point can result in significant mitigation of the MBI in bunches suitable for EEHG operation at FLASH2020+. Further, the results suggest that mitigation of the MBI can also be achieved by increasing the bunch energy spread by an amount well within the projected range of the new laser heater. Using a semi-Lagrangian simulation code for these studies allowed to calculate accurate linear and non-linear gain functions.

REFERENCES

[1] E. L. Saldin, E. A. Scheidmiller, and M. V. Yurkov, "An analytical description of longitudinal phase space distortions in magnetic bunch compressors", *Nucl. Instr. and Meth. A* vol. 483, pp. 516–520, 2002. doi:10.1016/S0168-9002(02)00372-8

ISBN: 978-3-95450-227-1 ISSN: 2673-5490 doi:10.18429/JACoW-IPAC2022-WEPOMS037

[2] D. Ratner *et al.*, "Time-resolved imaging of the microbunching instability and energy spread at the Linac Coherent Light Source" *Phys. Rev. ST Accel. Beams*, vol. 18, 030704, 2015. doi:10.1103/PhysRevSTAB.18.030704

[3] "FLASH2020+ - Upgrade of FLASH: conceptual design report", Verlag Deutsches Elektronen-Synchrotron DESY Hamburg, 2020. doi:10.3204/PUBDB-2020-00465

[4] SelaV, https://selav.desy.de

[5] Ph. Amstutz and M. Vogt, "A time-discrete Vlasov approach to LSC-driven microbunching in FEL-like beam lines", World Scientific, *Nonlinear Dynamics and Collective Effects in Particle Beam Physics*, pp. 182-191, 2019. doi:10.1142/9789813279612_0016

[6] R. L. Warnock and J. A. Ellison, "A general method for propagation of the phase space distribution, with Application to the Saw-Tooth Instability", World Scientific, *The Physics of High Brightness Beams*, pp. 322-348, 2000. doi:10.1142/9789812792181_0020

[7] C. Gerth *et al.*, "Layout of the laser heater for FLASH2020+", in *Proc. IPAC'21*, Campinas, Brazil, May 2021, pp. 1647–1650. doi:10.18429/JACoW-IPAC2021-TUPAB111

[8] E. L. Saldin, E. A. Scheidmiller, and M. V. Yurkov, "On the coherent radiation of an electron bunch moving in an arc of a circle" *Nucl. Instr. and Meth. A* vol. 398, pp. 373–394, 1997. doi:10.1016/S0168-9002(97)00822-X

[9] M. Venturini, "Microbunching instability in single-pass systems using a direct two-dimensional Vlasov solver", *Phys. Rev. ST Accel. Beams*, vol. 10, 104401, 2007. doi:10.1103/PhysRevSTAB.10.104401